# Chapter 1

# Introduction

Decentralisation of wireless control and data sharing systems allows flexible deployment structures over large areas. Conversely, using a single centralised node, deployments are limited by that node's placement and its maximum communication range. This paper studies the application of LoRa, an emerging long range, low power, radio frequency (RF) technology, for the decentralised use case of sparse robot swarms. Solutions are targeted at, and scenarios are devised from, the use case, however as the research topics discussed are applicable to many areas, descriptions are largely kept agnostic.

Swarm robotics is the coordination of multi-robot systems such that a common goal can be achieved. Capabilities of a swarm should exceed that of any single robot in the swarm; be that attributed to increased coverage [1] or self-assembly methods [2]. Although spreading robots across large areas opens up potential for many practical applications, including terrain mapping, and search and rescue, the sophistication of robots required in these real-world scenarios can make them prohibitively expensive, which can lead to limited robot density. These are referred to as sparse swarms.

Unlike a centralised control approach, swarms rely on robots sharing data directly so that all instances can build a combined interpretation of the environment. Although some data may need to be decimated to many or all robots in the network for purposes such as swarm management, the vast majority will only be of interest to physically local neighbours. Local interest data may be found obstacles or robot routes. In critical scenarios, for example when robot failure is impending, large fast data dumps may be required. Alternatively, data can be continuously aggregated and distributed in a BitTorrent-like fashion [3].

For concentrated deployments, these scenarios are trivial to implement using high-data-rate technologies such as Wi-Fi. However, in a real-world scenario, when inter-robot distance is significant, and there are line of sight (LOS) obstructions (e.g. trees), an alternative physical medium is required. This leads to the choice of LoRa, detailed in Section 2.1. The system can be considered as a mobile-ad-hoc-network (MANET), due to the ever changing topology caused by internal system changes (e.g. robot movement), or external system changes (e.g. weather).

Although LoRa is fundamentally ideal for long-range applications and operates in the low attenuation Sub-1GHz band, scenario specific conditions of ground-level transmissions and high-propagation environments are not ideal for RF communications. Therefore this project initially covers real-world testing in free-space and forests to assess how sparse swarm deployment scenarios may affect LoRa's physical radio performance. From this, demodulation models are extracted and combined with LoRa collision models from literature to create a simulator for testing LoRa ad-hoc scenarios. This simulator is used to analyse the effectiveness of three MAC protocols with the aim of distributing local-interest data to physically local neighbours. Two methods utilise common approaches (ALOHA and CSMA), and the third attempts to exploit hardware parameters and regional RF regulations; this is defined as the LoRa Local Broadcast Protocol (LLBP).

# Chapter 2

# Background

## 2.1 LoRa

### 2.1.1 Overview

LoRa is a physical long-range, low-power, communication technology developed and patented by Semtech[1]. It is designed to operate inside unlicensed Sub-1GHz ISM bands worldwide. Consequently, it can be used for wide area deployments without being tied to expensive licensed carriers (see Section 2.2). Fundamentally, even using its fastest configuration, it is a low-data rate modulation technique.

Long-range communication in the ISM bands is challenging as heavy congestion can result in a high physical noise floor; that is the sum of all signals in the band from sources such as the atmosphere or radio devices, excluding the wanted signal. LoRa functions using a unique spread spectrum modulation technique that allows signal-to-noise degradation in a single channel to be compensated for by spreading across other channels, meaning signals can be received below the noise floor. As the spreading amount can be changed, LoRa modulation boasts a high and adaptive sensitivity. This adaptability allows LoRa to make far more efficient use of its link budget compared to frequency shift keying (FSK) and other modulation types [4]. The link budget being the measure of all gains and losses incurred by a signal passing through the transmitter, the receiver and said propagation channel. A system is said to be link limited when channel losses result in a receive power (and therefore SNR)

---

[1]Semtech, USA, https://www.semtech.com/

lower than can be demodulated by the receiver. Equation 2.1 identifies the link-budget in its simplest form.

$$RX \; Power \; (dB) \; = TX \; Power \; (dB) \; + \; Gains \; (dB) \; - \; Losses \; (dB) \qquad (2.1)$$

## 2.1.2   Parameters

LoRa hardware has many parameters that can be configured to extend range or increase reliability at the expense of airtime, data-rate or energy consumption. These are independent from any external hardware and include:

- **Bandwidth (BW)**: The range of the chirps around the CF. Increasing bandwidth increases data-rate but decreases receiver sensitivity [5].

- **Carrier Frequency (CF)**: The centre frequency of chirps. Current hardware targets some sub-range of 137MHz to 1020MHz at a resolution of 61Hz [6].

- **Coding Rate (CR)**: The amount of redundant information encoded in symbols for forward error correction (FEC); trade-offs can be seen in Table 2.1. FEC is most effective in the presence of burst interference [4].

- **Preamble Symbols (PSs)**: The number of programmed preamble symbols sent for receiver synchronisation. Packet receive percentage (PRP) has been shown to increase with increased PSs up to a threshold [7]. CAD performance also improves with PS count (see Section 2.1.5).

- **Spreading Factor (SF)**: The ratio of chip rate to bit rate, where chips per symbol is given as $2^{SF}$. Receiver sensitivity increases in line with spreading factor [6]. The trade-offs can be seen in Table 2.2.

- **Transmission Power (TP)**: The radio output power. Equation 2.1 highlights how an increased TP directly increases link budget with the obvious drawback of higher power usage.

Selection of these parameters is often manual, however mechanisms such as LoRaWAN's adaptive data-rate (ADR) [8], or "probing algorithms", as proposed by [9], can be used to choose these parameters such that transmission energy is reduced whilst maintaining an adequate throughput and link budget. LoRaWAN abstracts SFs and BWs into a set of orthogonal data-rates (DRs) to simplify selection, where lower data-rates have higher range [10]. It has been suggested that ADR

has low-scalability due to packet count requirements [11] and is slow to converge [12]. Likewise [9] requires a large number of initial transmissions, making both only suitable for static nodes in a gateway controlled network.

TABLE 2.1: Effect of CRs on LoRa transmissions. Recovery performance is defined as the best case percentage of bits that can be lost for a successful receive. Compiled from data in [7].

| Coding Rate | Data Overhead | Recovery |
|:---:|:---:|:---:|
| 4/5 | ×1.25 | 20% |
| 4/6 | ×1.50 | 33% |
| 4/7 | ×1.75 | 43% |
| 4/8 | ×2.00 | 50% |

TABLE 2.2: Effect of SF on LoRa transmissions (BW=125KHz). Compiled from data in [4] and [7].

| SF (LoRa Mode) | SF (Chips / Symbol) | Bit Rate (bits / sec) | Demodulation Limit (SNR dBm) |
|:---:|:---:|:---:|:---:|
| SF7 | 128 | 5469 | -7.5 |
| SF8 | 256 | 3125 | -10.0 |
| SF9 | 512 | 1758 | -12.5 |
| SF10 | 1024 | 977 | -15.0 |
| SF11 | 2048 | 537 | -17.5 |
| SF12 | 4096 | 293 | -20.0 |

## 2.1.3 Airtime

To understand a configuration's performance, it is critical to know its airtime; this defines bitrate and affects channel contention methods. The total airtime of a transmission (Equation 2.3) is dependent on the number of symbols being transmitted (Equation 2.2) and the time each symbol takes to send. Preamble and payload are calculated individually as it can be useful to consider them as separate components for purposes such as CAD. Equations are adapted from [6] to suit the notation and

formats used by this paper.

$$S_{preamble} = \text{PS} + 4.25 \tag{2.2a}$$

$$S_{payload} = 8 + \max\left(\text{ceil}\left[\frac{8\text{PL} - 4\text{SF} + 16\text{CRC} + 20\text{EH} + 8}{4(\text{SF} - 2\text{LDR})}\right]\frac{1}{\text{CR}}, \ 0\right) \tag{2.2b}$$

$$S_{total} = S_{preamble} + S_{payload} \tag{2.2c}$$

The unmentioned factors in Equation 2.2 are: the number of bytes in the packet (PL), whether the CRC check is enabled (0 or 1), whether the explicit header (EH) is enabled (0 or 1) and whether low-data-rate optimisation (LDR) is enabled (0 or 1). LDR is used when $T_s > 16\text{ms}$ to aid stability over long transmits [6].

$$T_s = \frac{1}{S_R} = \frac{2^{\text{SF}}}{\text{BW}} \tag{2.3a}$$

$$T_{preamble} = S_{preamble} \cdot T_s \tag{2.3b}$$

$$T_{payload} = S_{payload} \cdot T_s \tag{2.3c}$$

$$T_a = T_{packet} = T_{preamble} + T_{payload} \tag{2.3d}$$

Equation 2.3 highlights that each SF increment will cause $T_a$ to double for the same number of symbols. Likewise, doubling BW will half $T_a$. Figure 2.1 shows the structure of a LoRa transmission and therefore where each airtime component comes from.
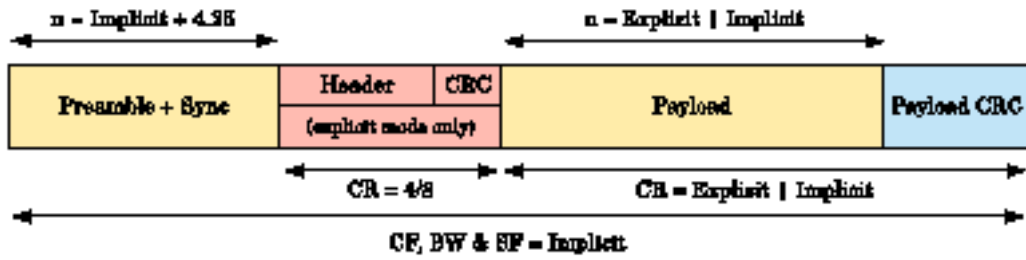


FIGURE 2.1: LoRa transmission structure. All transmissions contain a preamble, sync words, and a payload. The header section (in red) is optional but if present, contains information such as the payload length, the payload CR, and whether the CRC is present. If the header is not present this information must be fixed implicitly by the receiver. Parameters that are not in the header are always implicit and must match between transmitter and receiver. Adapted from [6].

## 2.1.4  Receive Behaviour

LoRa radios, like all consumer radios, are half-duplex, meaning they are unable to receive for the duration of transmissions. Additionally, end device radios will usually be transceivers, which can only demodulate one incoming signal at a time [6]. In the presence of multiple signals, some transmissions may be missed, or collisions may occur, causing all transmissions to be missed. Collision scenarios specific to LoRa are identified in Table 2.3.

TABLE 2.3: Collation of LoRa collision scenarios as defined by [13] and [14]. [14]'s definition of the important preamble (IP) is used: the four fixed preamble symbols and proceeding two symbols of the programmed preamble. Situations use two transmission sources (A and B) and one receive source (C).

| ID | Time | Power | C Result |
|----|------|-------|----------|
| A | $B_{start} > A_{\text{IP}}$ | $A_{\text{RPS}} \geq B_{\text{RPS}}$ | Receives A |
| B | $B_{start} > A_{\text{IP}}$ | $A_{\text{RPS}} < B_{\text{RPS}}$ | Receives A |
| C | $B_{start} > A_{\text{IP}}$ | $A_{\text{RPS}} \ll B_{\text{RPS}}$ | CRC Fail A |
| D | $B_{start}\ inside\ A_{\text{IP}}$ | $A_{\text{RPS}} \leq B_{\text{RPS}}$ | Collision |
| E | $B_{\text{IP}} \approx A_{\text{IP}}$ | $A_{\text{RPS}} \approx B_{\text{RPS}}$ | Collision |
| F | $B_{\text{IP}} \approx A_{\text{IP}}$ | $A_{\text{RPS}} \gg B_{\text{RPS}}$ | Receives A |

It should be noted that a different technology exists in gateways (a LoRa concentrator block), allowing demodulation of up to eight signals concurrently, provided they use unique spreading factors [15]. Although gateways are clearly more powerful than transceivers, their cost and power usage make them hard to deploy on scale. However, Pycom's[2] newly released Pygate gateway is a fraction of the cost of existing implementations and may be feasible for ad-hoc scenarios.

Most LoRa applications consist of many sensor nodes infrequently sending data on different spreading factors to a single gateway with very little downlink present; this means collisions and missed receives are rare. Unfortunately, in ad-hoc networks, these events are very likely; this is explored in Section 2.3.2.

---

[2]Pycom, UK, https://pycom.io/

## 2.1.5    Channel Activity Detection (CAD)

Carrier-sensing is a helpful mechanism for radios to check whether a channel is busy
or idle. Usually, this is achieved by checking the power present in the channel using
the received signal strength indicator (RSSI). This is a very unreliable method for
LoRa because the RSSI includes channel noise, and LoRa signals can operate below
the noise floor. For this reason, LoRa radios offer a specialised CAD method, which
searches the channel for a single preamble symbol. CAD is at least 97% reliable in
the presence of preamble with false positives occuring just 0.1% of the time [13]. It
has been shown that CAD can in fact detect non-preamble symbols when there is
high signal strength, although this ability quickly becomes unreliable in a real world
scenario [16].

## 2.1.6    Signal Orthogonality

The manner of LoRa's modulation allows multiple signals to co-exist in the same
channel provided they have a different chirp rate, where $C_R = \text{BW} \cdot S_R$, otherwise
written as $C_R = \frac{\text{BW}^2}{2^{\text{SF}}}$. This clearly demonstrates that for a single bandwidth, all
SFs must be orthogonal to one another. However, in the case that different BWs
are used, different SFs may have the same chirp rate and could interfere; this is
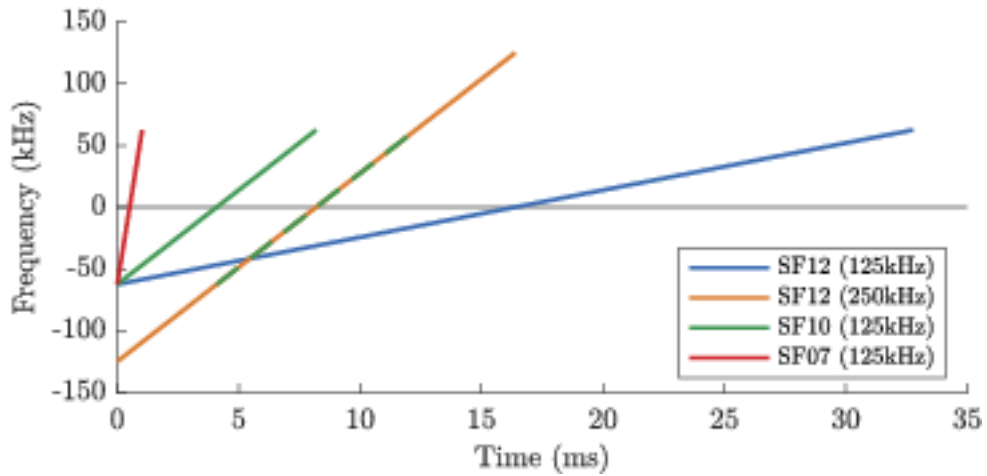demonstrated in Figure 2.2.



FIGURE 2.2: Demonstration of signal orthogonality for different SFs. The SF10
125kHz chirp is duplicated and shifted to overlap with the SF12 250kHz chirp to
highlight that they have the same chirp rate and are therefore not orthogonal.

## 2.2   ISM Band Regulation

The industrial, scientific and medical (ISM) bands are portions of the radio spectrum, which can be used without a license, subject to local regulatory standards. These standards vary around the world but often define maximum power outputs, duty cycles (DCs), and bandwidths. Though limits can be problematic, they help reduce the chance of internal and external system interference. Some of the most stringent regulations are in Europe, where they are controlled firstly by the ETSI[3], and then by country specific authorities. The United States' regulations are managed by the FCC[4], with many other countries following their example.

Sub-1GHz LoRa hardware operates around the 433MHz and 900MHz bands, but as the former is very heavily regulated for ad-hoc scenarios in the US [17], only the 900MHz area is considered viable. It should be noted that the specific available frequencies still differ between region, as is demonstrated by LoRaWAN's use of the 863-870 MHz and 902-928 MHz bands for Europe and the US respectively [10]. A comparison of the regulations can be seen in Table 2.4. As ETSI limits vary heavily on a by band basis, they are broken down further in Table 2.5.

TABLE 2.4: Regional regulation comparison for 900MHz band radio [18], [19].

|  | FCC | ETSI |
|---|---|---|
| **Band** | 902–928MHz | 863–870MHz |
| **EIRP** | 36dBm | 0.25MHz @ 27dBm |
|  | *30dBm transmit power* | 6.40MHz @ $\leq$ 14dBm |
| **Duty Cycle** | None | 0.1%–10% |
| **Bandwidth** | 26 MHz | 6.65MHz |
| **Narrowband** | 400ms airtime per transmit | None |
| **CSS** | None | Varies |

DC limits greatly reduce the amount of airtime a radio is allowed. For example, in Band h1.3, there is a 1% DC, which indicates a maximum of 36 seconds of airtime, over all the band's channels, over a rolling one hour period. DCs are considered within a band so a multi-band implementation may obey multiple DCs separately.

---

[3]ETSI, EU, https://www.etsi.org
[4]FCC, US, https://www.fcc.gov

Alternatively, the polite spectrum access (PSA) policy can be used. PSA allows
airtime of up to 100 seconds per 200kHz of spectrum, per hour, regardless of DC
[20]. It does however require a clear channel assessment to be carried out before
every transmission, independent of LoRa's CAD.

TABLE 2.5: ETSI 868MHz sub-bands for short range devices (adapted from [19]).
Only bands relevant for CSS are included. Band numbers correspond to CEPT-
ERC-REC 70-03 definitions [21]

| Band | Frequency (MHz) | EIRP (dBm) | DC | Max BW (kHz) |
|---|---|---|---|---|
| h1.2 | 863.00–870.00 | 14 | 0.1% | 7000 |
| h1.3 | 865.00–868.00 | 14 | 1% | 300 |
| h1.4 | 868.00–868.60 | 14 | 1% | 600 |
| h1.5 | 868.70–869.20 | 14 | 0.1% | 500 |
| h1.6 | 869.40–869.65 | 27 | 10% | 250 |
| h1.7a | 869.70–870.00 | 7 | None | 300 |
| h1.7b | 869.70–870.00 | 14 | 1% | 300 |

Regulations consider power as equivalent isotropically radiated power (EIRP). This
value is directly related to radio transmission power and can be calculated as EIRP =
$TP - L + G$ where $L$ is cable loss and $G$ is antenna gain. The latter occurring from the
antenna concentrating transmit power into a smaller. This means a radio operating
in Band h1.3, using a typical omnidirectional antenna with 3dBi of gain, can only
transmit at 11dBm if no cable loss occurs. Directional antenna compound these
issues due to their high-gains and the low EIRP limits.

The ETSI regulations are the limiting factor in transmit power, DC and overall
available bandwidth. LoRa being a CSS signal means FCC narrowband limitations
need not be a concern. Under this consideration, the ETSI regulations are used as
the worst-fit scenario from here on in. When considering national regulation, it is
common that either all bands are implemented, or none at all [21]. Of the ETSI
bands, h1.3, h1.4 and h1.6 are of most interest. h1.3 and h1.4 giving a balanced
offering of bandwidth, EIRP and DC. Whilst h1.6 offers a far greater DC and EIRP
but limited bandwidth; a further regulatory limit means only allows a single wide-
band channel can operate within this band. The maximum number of possible LoRa
channels in each of these bands can be seen in Table 2.6.

TABLE 2.6: Maximum channel count breakdown for relevant ETSI bands, calculated for LoRa's most common operating bandwidths with channel spacing 120% of the BW (to avoid inter-channel interference).

|        | Channel BW | | |
| :---: | :---: | :---: | :---: |
| **Band** | **125kHz** | **250kHz** | **500kHz** |
| **h1.3** | 19 | 8 | N/A |
| **h1.4** | 4 | 2 | 1 |
| **h1.6** | 1 | 1 | 0 |

# 2.3   Ad-Hoc Networks

## 2.3.1   Routing

An ad-hoc network is a type of wireless network that does not rely on managed infrastructure. The network's nodes are responsible for determining their own routing paths and forwarding other nodes packets (i.e. acting as the routers). A MANET, is a type of ad-hoc network where nodes are expected to move, resulting in frequent changes to the network topology [22]. If a network is sparse or operating at the limits of the transmission medium, and packet delivery is not time critical, the network can be treated as a delay-tolerant-network (DTN). A common approach is to adopt store-carry-forward (SCF) behaviour; this is where intermediate nodes will keep hold of data until either a new path appears or signal strength improves [23]. A major requirement of ad-hoc networks, and the most researched topic, is route management [24]. However, as this paper focuses on local broadcasts, the topic is not considered further, instead the reader is directed towards [25].

## 2.3.2   MAC Protocols

An ad-hoc network contains many transmitters, therefore a medium access control (MAC) protocol is required to regulate access to the shared transmission medium. The selected method has a considerable effect on network efficiency in terms of collision occurrence, throughput and fairness. Protocols can be classed as either contention-free or contention-based. The former use transmission schedules; these struggle to adapt to changing topologies, and can waste resources if nodes do not

require equal access, but can be completely collision-free. The latter rely on nodes competing for access, these are flexible as they can adapt to different topologies with little overhead, however they are not collision free. For critical communications it must be possible to detect these collisions and recover from them. This can be very costly, requiring acknowledgements and retransmissions [26].

IEEE 802.11 (Wi-Fi) uses a combination of carrier-sense multiple access (CSMA) and multiple access with collision avoidance (MACAW). This is where a node first senses the medium for activity, before reserving the channel by transmitting control messages [27]. Theoretically this will alert other nodes so they do not transmit for this duration. Although the overhead introduced is not ideal, it is acceptable for high data-rate communications and large transmissions. The reservation phase is inefficient for LoRa due to its long airtimes, however, pure carrier sensing implementations using LoRa's CAD have been shown to be effective in the presence of receivable transmissions [16].

LoRaWAN is a MAC protocol designed to be the de facto choice for point-to-multipoint LoRa applications. It is largely certified worldwide, and is both managed and promoted by the LoRa Alliance[5]. The expectation of a star topology means the full protocol is not suited to ad-hoc scenarios, however, individual features are of interest. In principle it is implemented as P-ALOHA, a simple unchecked protocol where transmission occurs whenever a transmitter has data available to send. DC limits play a large part in keeping collisions at a minimum, Figure 2.3 explains how these are enforced. The unchecked approach reduces theoretical channel usage to just 18% [28]. [29] attempts to apply ad-hoc routing to LoRaWAN, however, due to the low-data-rate nature of LoRa, the implementation largely relies on gateways linked via the internet.
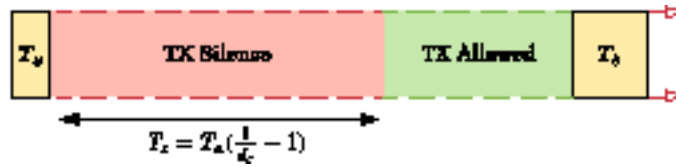


FIGURE 2.3: Demonstration of how LoRaWAN enforces duty cycle limits; that is after a transmission of airtime $T_a$, the transmitter must be silent for a minimum period of $T_s = T_a(\frac{1}{d_c} - 1)$ [30]. The figure is to scale for $d_c = 10\%$.

# Chapter 3

# LoRa PHY Testing

It has been repeatedly shown that LoRa transmissions can be received at distances exceeding 10km in unobstructed environments (free-space) when antennas are highly elevated [31]. However, these ideal radio conditions are unrealistic for swarm robots operating close to the ground in high-propagation environments such as forests. Therefore the first experiment in this paper identifies LoRa's physical performance and scenario specific limitations. Due to expected sparsity, only far field scenarios are relevant ($d_{\mathrm{SP}\leftrightarrow\mathrm{MP}} > 0.35$m).

## 3.1    Methodology

The purpose of this testing was to inform protocol decisions and assess capability of an off-the-shelf LoRa PHY. A focus was taken to get enough data across a small selection of important scenarios and parameters to allow quantitively assessment.

The two main transmission environments selected were free-space and in-forest; this was to give an understanding of both low-propagation and high-propagation scenarios. Data collection was mainly spread over two locations: $L_A$ and $L_B$ (split into $L_{B1}$ and $L_{B2}$), identified in Figure 3.1 and 3.2 respectively. All locations were rural and therefore theoretically free from strong sources of external interference. Radio placement was decided by first placing the transmitting radio (slave) at a fixed location (SP), and then, using the furthest receivable point as the starting point for the receiving radio (master). From there the master was positioned closer towards the slave for each future test (MP). In each scenario the main interest was ground level transmissions; however, to assess whether radio performance was

actually compromised by the placement, comparative measurements were taken with an elevated antenna.
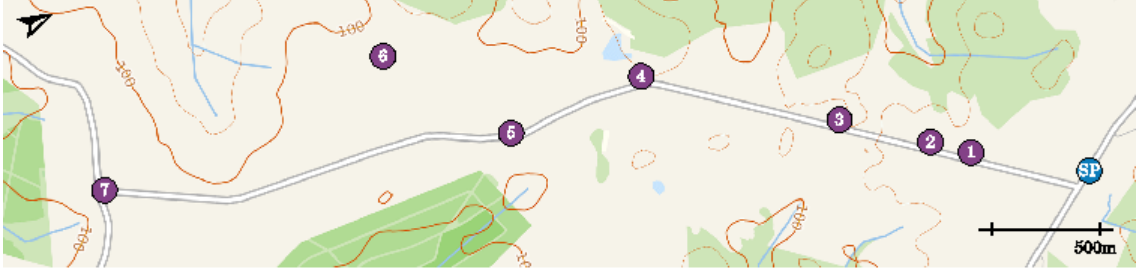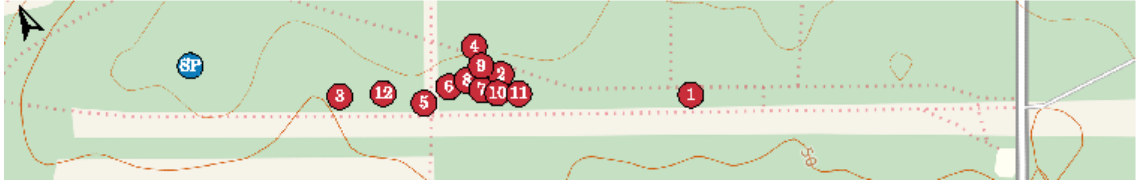


FIGURE 3.1: Test positions for $L_A$ : The New Forest, Hampshire, UK.[1]
SP in open with LOS to other points a combination of free-space and light vegetation. Exact positions are in Appendix B.1. To the left of MP7 vegetation density increases, making MP7 the furthest position viable for free-space testing.



(A)  Test positions for in-forest testing ($L_{B1}$). SP in forest with LOS to other points continually obstructed by a combination of leaved and bare trees. Exact positions are in Appendix B.3. Large clump of MPs where radio reception was inconsistent.
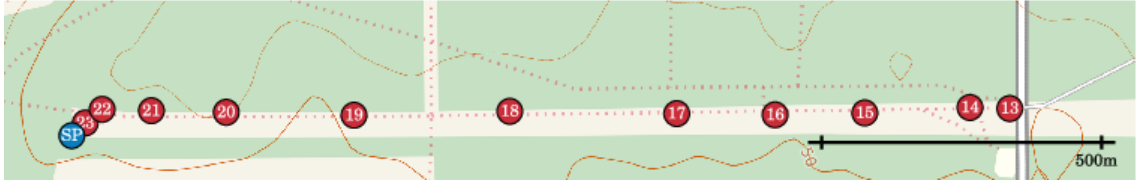


(B)  Test positions for free-space testing ($L_{B2}$). SP in open with LOS completely free-space. Exact positions are in Appendix B.2. No access to right of MP13.

FIGURE 3.2: Test locations for $L_B$ : Stansted Forest, West Sussex, UK.[1]

In terms of radio parameters, SF was the main focus due to it being an option mostly unique to LoRa; all values were tested for this in all locations (SF = 7, 8, 9, 10). Variations using the lowest (4/5) and highest (4/8) CRs were collected to verify FEC performance. Additionally, as the maximum transmission unit is often defined by the protocol, the effects of varying packet length were taken (PL = 20,

128, 255 [PHY limit]). The rest of the parameters were fixed. The 868.1MHz CF was used with TP set to 14dBm so that collected data would be relevant in regard to ETSI regulations. The bandwidth was fixed to 125kHz so that radio sensitivity was only affected by the SF. The PSs were set to 8 to match LoRaWAN [10]. The number of packets (PC) transmitted for each configuration was set to 50; though not guaranteed, this gave reasonable expectation of a normal distribution. See Table A.1 for full test definitions.

To test the point-to-point transmissions, two identical platforms, which together could log the performance of sending and receiving LoRa transmissions, were required. The platforms had to be suitable for outdoor use, be able to test multiple radio configurations whilst on location and provide a mechanism to indicate to user when the maximum range had been reached. The hardware and corresponding software created for this purpose is detailed in Appendix C.



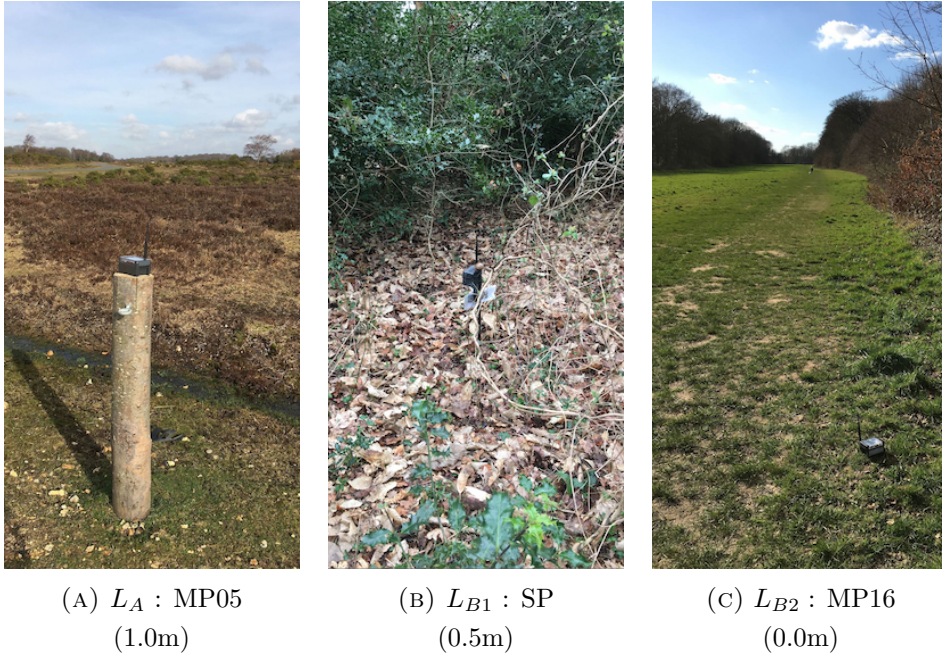(A) $L_A$ : MP05 (1.0m)      (B) $L_{B1}$ : SP (0.5m)      (C) $L_{B2}$ : MP16 (0.0m)

FIGURE 3.3: Pictures of test environments and conditions. Although testing was split across multiple days at each location, the same dry conditions were present.

## 3.2    Results & Discussion

In total 498 test cases were executed, totalling 24,900 packet transmissions. Of this
total, 19,545 were successfully received (78.5%). The distribution of receive condi-
tions for these individual points is indicated by Figure 3.4. When discussing results,
received packets are considered alongside all other packets from the corresponding
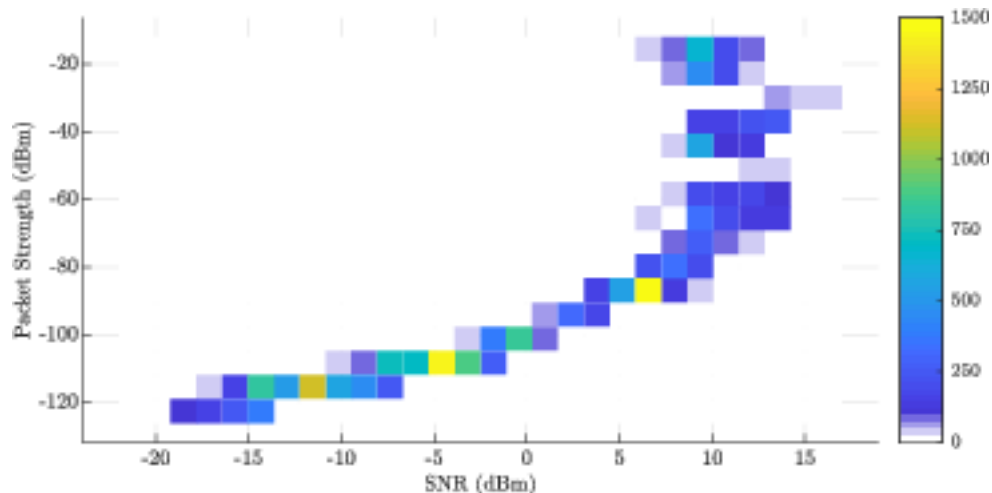TD; allowing for packet receive percentage (PRP) and average SNR metrics.



FIGURE 3.4:   Density plot of received packet transmissions modelled as a bi-
variate histogram with colour indicating received packet count.
$Total\ \ Points = 19,545$

Results are considered in two domains: the demodulation performance of the radio,
and the environment effects. This is done because, even though actual receive perfor-
mance varies with factors such as distance and attenuation, these can be abstracted
into changes of the underlying SNR and RPS figures seen by the receiver. As there
are no other transmission sources in this testing, theoretically, if these figures are
within the required bounds for demodulation success, receives are successful.

### 3.2.1    Demodulation Performance

When SNR $\leq$ 0 the RSSI value indicates the amount of noise seen by the receiver in
the presence of no packet. When operating at 868MHz, the noise that the receiver
should see is approximately the thermal noise floor $(-174 + 10 \log_{10}(\mathrm{BW}))$, plus the
receiver noise figure; LoRa implementations should have a noise figure of around
6dBm [4]. This indicates that for a 125kHz receive, the noise floor $(n_f)$ should be
-117dBm.  The empirical noise floor calculated across all locations was -103dBm

with a standard deviation of -109dBm; this is 14dBm (24×) higher than expected. As the variance is low, this result indicates that the RFM95W hardware is of much poorer quality than expected, with a noise figure of 20dBm.

Whether the radio receives a transmission is dictated by whether the received power exceeds the receiver sensitivity ($R_S$). For LoRa modules, $R_S = n_f - D_L$, where $D_L$ is the minimum SNR required for the current SF (see Table 2.2). This performance is explored in Figure 3.5 and 3.6. In short, performance is close to theoretical for SF = $7, 8, 9, 10$ but SF = $11$ & $12$ perform similarly to SF = $10$ with higher reliability. For all configurations, receive success is highly variant when approaching the empirical sensitivity.
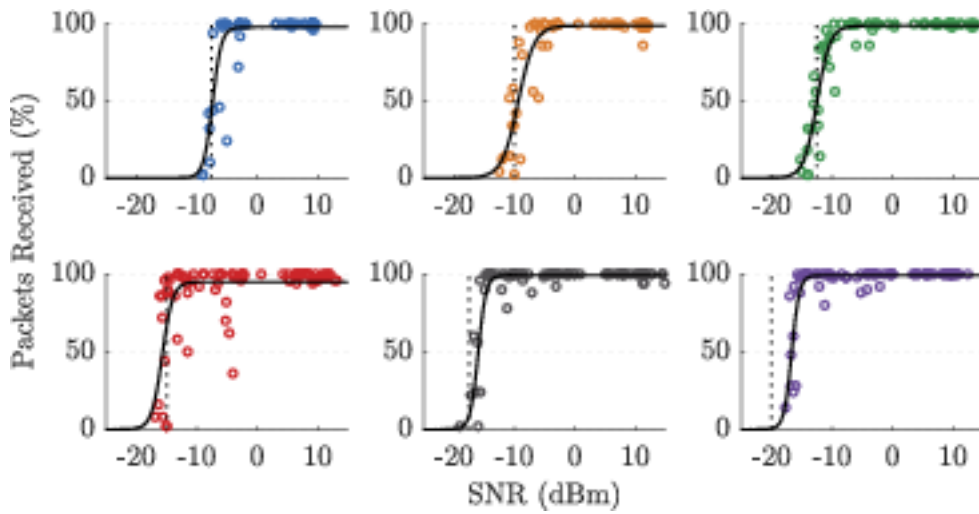


FIGURE 3.5: TD mean SNR values plotted against their PRPs, separated by SFs (Order = [[7, 8, 9], [10, 11, 12]]). For each SF plot: $D_L$ is indicated by the dotted line and the solid line corresponds to the best-fit sigmoid function; these are repeated in Figure 3.6. Although the best-fits give a good representation of the general data pattern, and provide empirical demodulation cut-offs, they do not capture the high-variance receive behaviour when approaching the cut-off. This is reflected by: 62%, 60%, 66%, 39%, 77% and 82% of the respective training points fall inside the corresponding 95% confidence interval.

Theoretically, higher CRs will result in more data being recovered from a transmissions allowing for greater receive success. Comparative tests are plotted in Figure 3.7. As no strong visual conclusions can be made, a null hypothesis is proposed; $H_0$ : *The mean PRP does not increase between receives using CR 4/5 and CR 4/8* (otherwise written as $4/5_{\mathrm{PRP}} \geq 4/8_{\mathrm{PRP}}$). The respective means are 71.8% and 72.5%. Using a left-tailed Wilcoxon signed rank test for non-normal distributions gives $p = 41.2\%$. With a 5% significance level, $H_0$ cannot be rejected, indicating that CR has no effect on PRP. Given that the SNRs are not significantly different

*(hypothesis testing omitted)* this indicates that receive drop-off and high variance when approaching sensitivity limits is the limiting factor for demodulation. The lack of CR effect is unsurprising given that FEC's main performance should be seen in the presence of burst interference.
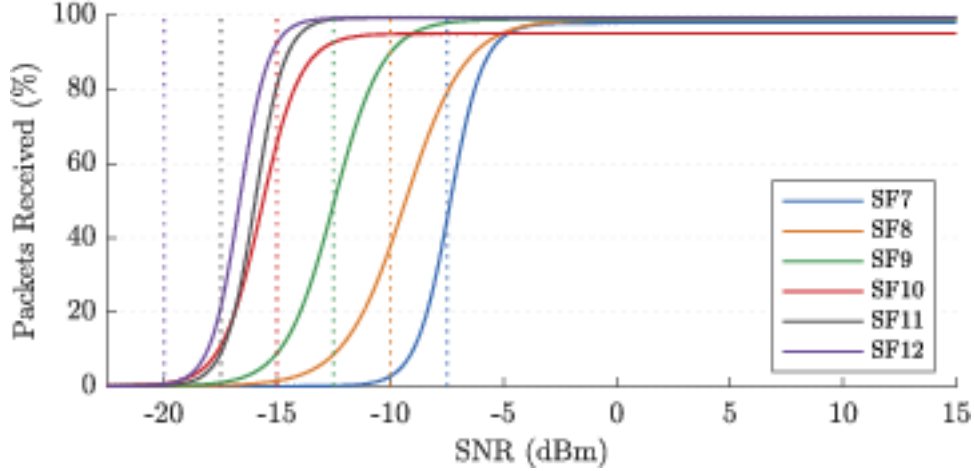


FIGURE 3.6: Plot of sigmoid best-fits generated in Figure 3.5. The plot clearly demonstrates the positive effect increasing SF has on demodulation performance of the receiver. For SF $= 7, 8, 9, 10$ demodulation success starts dropping approximately 2.5dBm before $D_L$, with a 50% PRP at $D_L$. This holds less so for SF=11, for which drop-off starts around $D_L - 5$dBm, until $D_L$ where there is only a 10% receive success. For SF=12 drop-off starts around $D_L - 7.5$dBm, until $D_L$ where there is a 0% receive success. Given the stable RSSI when SNR $< 0$, and that expected performance holds until a certain SNR, there is an indication that receiver sensitivity is not as high as stated.

When the amount of data increases in a packet, its airtime will increase for the same configuration; this can lead to more channel noise being introduced (lower SNR) and receiver clock drift (lower demodulation performance). The effect this has on comparative tests is plotted in Figure 3.8. The mean PRPs of PL $= 20, 128, 255$ are 81.7%, 78.8% and 76.8% respectively. Three null hypotheses are proposed: $H_0^1 : 20_\text{PRP} \leq 128_\text{PRP}$, $H_0^2 : 20_\text{PRP} \leq 255_\text{PRP}$ and $H_0^3 : 128_\text{PRP} \leq 255_\text{PRP}$. Using right-tailed Wilcoxon signed rank tests with 5% significance, $H_0^1$ ($p = 1.1\%$) and $H_0^2$ ($p = 0.0\%$) are rejected but $H_0^3$ ($p = 13.6\%$) is not. Therefore alternative hypotheses can be accepted $H_A^1 = 20_\text{PRP} \geq 128_\text{PRP}$ and $H_A^2 = 20_\text{PRP} \geq 255_\text{PRP}$. Given that the SNRs are not significantly different, and that $H_A^3$ is narrowly rejected, a loose relationship between increased PL and lower demodulation performance is assumed.
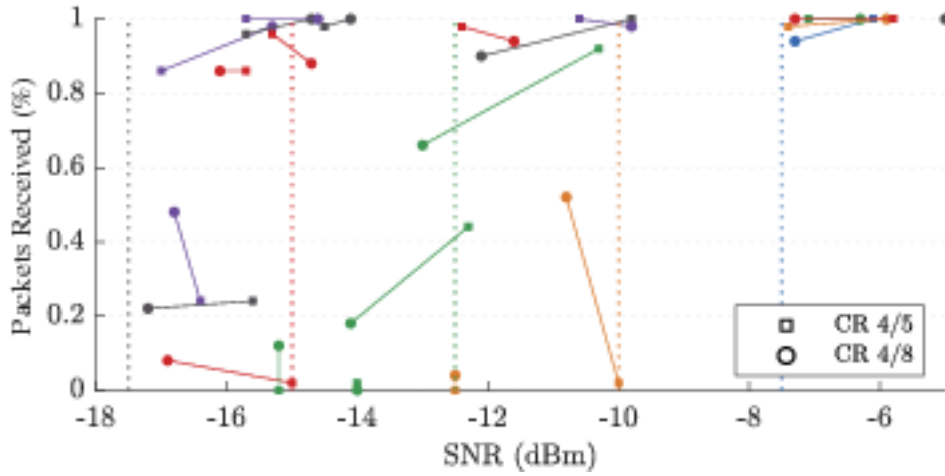
FIGURE 3.7: Plot of SNR and PRP for varying CRs. Only configurations where all other factors are identical are included (e.g. height, location, LoRa configuration). A line joins each set of points with a matching configuration. When SNR > −5, the PRP is nearly always 100% and is therefore excluded.
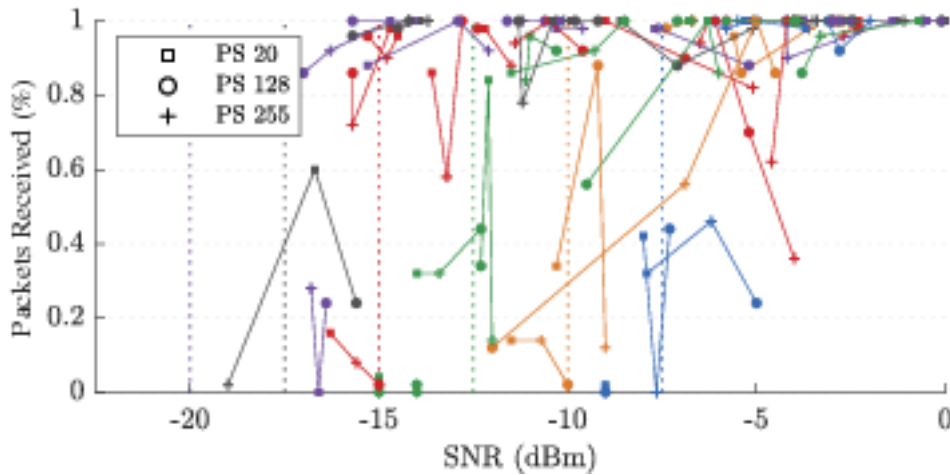


FIGURE 3.8: Plot of SNR and PRP for varying PLs. Only configurations where all other factors are identical are included. A line joins each set of points with a matching configuration. When SNR > 0, the PRP is nearly always 100% and is therefore excluded.

## 3.2.2 Environment Effects

Free-space is the least attenuating environment possible and as such a transmission in free-space should represent the minimum path loss over a given distance; directly leading to the maximum transmission distance. The minimum free space path loss (FSPL), is calculated as $20 \log_{10}(d) + 20 \log_{10}(f) - 27.55$ where $d$ is distance in meters and $f$ is frequency in MHz [32]. A more reasonable estimate must take into account effects such as ground reflection. The plain earth (PE) model considers

this and is calculated as $40\log_{10}(d) - 20\log_{10}(h_r) - 20\log_{10}(h_t)$ [33]. These are all plotted on Figure 3.9. Although transmissions occur at $0.0m$, receiver height $(h_r)$ and transmitter height $(h_t)$ are measured as the top of the antenna $(h_r = h_t = 0.17m)$. As neither model fits the test data, with FSPL underestimating and PE overestimating path loss, an empirical log-model is calculated as $91\log_{10}(d + 362) - 167$ (E-FSPL). This model fits the curve well but does not necessarily capture the variance caused by fading, as is reflected by only 83% of data points falling in the 90% confidence bound.
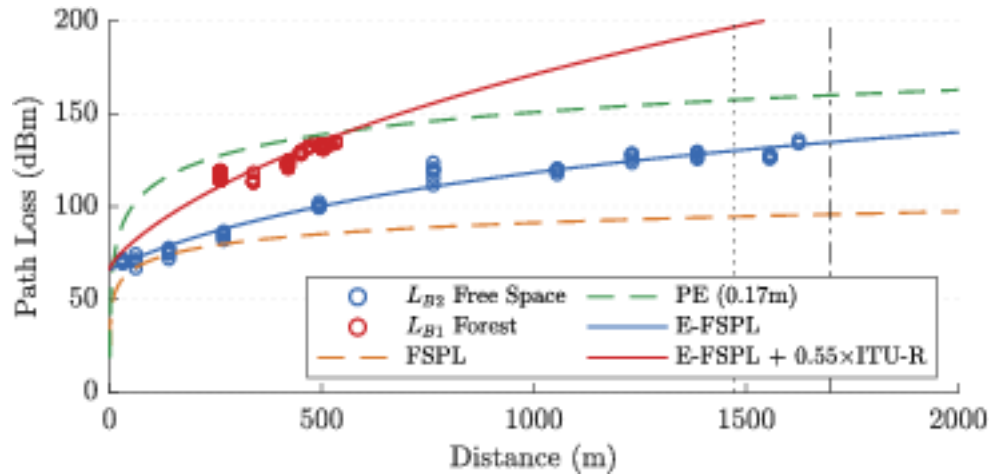


FIGURE 3.9: Plot of path loss for ground level transmissions through free-space $(L_{B2})$ and forest environments $(L_{B1})$. The LOS horizon and radio horizon are identified as the black dotted and dashed lines respectively.

Forests have high attenuation and should significantly increase path loss and reduce transmission distance. Due to the differences and complexity of vegetation, there is no de-facto propagation model, however, path loss should approximately match that of a vegetation model added to the environment's free space model [33]. Many are explained in [34], each of which can be made more flexible by applying an empirical multiplier, giving $L_{Total} = L_{FS} + \beta \times L_{Veg}$ [35]. The in-forest model demonstrated is the free-space-fit model with the ITU-R vegetation model, where $\beta = 0.55$. The model fits the in-forest test data; giving confidence in both the free-space fit model and that in-forest behaviour follows that of generalised RF transmissions. Inter-transmission variance for a single test can be attributed to fading, however, it should be noted that test execution was inconsistent when approaching the transmission limit. This is likely a result of the bearing change between transmitter and receiver causing significant changes to the LOS obstacles. To model this, either individual objects could be modelled or a varying empirical multiplier could be used. Although both the free-space and in-forest fit models serve the purpose of describing the test data, a full assessment of their generalisation would require significantly more data.

Transmissions at 868MHz are classed as ultra-high-frequency and usually have a maximum distance somewhere between the visual-horizon and radio-horizon [32]. They are also susceptible to ground plane effects which can increase path loss. Varying radio heights for comparable measurements are plotted in Figure 3.10. The decrease in path loss is clearly seen for both 0.0m → 1.0m and 0.5m → 1.0m. The effect is less clear for 0.0m → 0.5m. In free-space with $d = 10$m on grass: path-loss for 0.0m, 0.5m and 1.0m is 67dBm, 64dBm and 44dBm respectively. The increase between 0.0m and 0.5m is mathematically significant but of an insignificant degree compared to 0.5m → 1.0m. These results are in-line with the principle that the ground effect is insignificant once antenna height is more than a few wavelengths [32]. It is probable that transmissions are limited by the horizon in free-space given that the furthest receivable transmissions occur between the horizons for both 0.0m and 0.5m and there is sudden increase in path loss between the horizons for 0.0m.
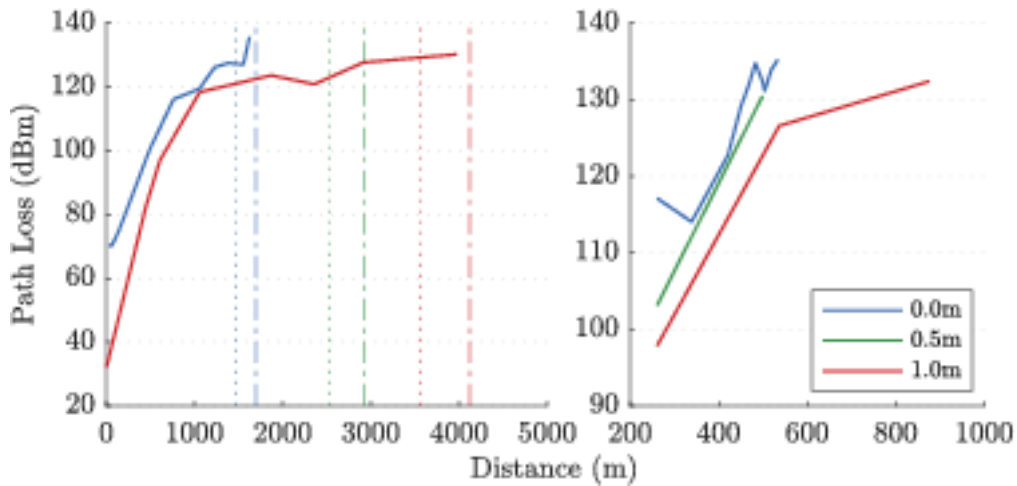


FIGURE 3.10: Plot of path loss for varying heights in free-space (left) and in-forest (right). Path loss is the mean of all tests at location. The dotted lines identify the LOS horizons. The dashed lines identify the radio horizons. Directly comparable data was not recorded for free-space 0.5m over multiple distances.

Overall range results indicate that LoRa is suitable for single-hops in a system with sparsely separated radios; ranges of 500m can be expected for SF = 11 regardless of the propagation environment. However, even with the 1600m range offered in free space, single-hop point-to-point coverage to all radios is unlikely, leading to the expected dynamic mesh topology.

# Chapter 4

# LoRa Ad-Hoc Simulator

This section proposes a specialised LoRa ad-hoc simulator, using models directly from PHY testing, as well as literature, to allow assessment of protocol performance. It supports both scripted access for statistical testing and a GUI overlay for visually identifying system behaviour and performance.

## 4.1   Model

### 4.1.1   Overview

The model is considered as three main components, the environment, the radios, and time. The environment is responsible for understanding radio placement and the propagation channel between radios. Radios create new transmissions and poll the environment for existing transmissions, which they then attempt to receive. The simulator supports both the theoretical LoRa radio (modelled from the datasheet), and the empirically defined RFM95W. Time progression of the system is modelled using the activity-oriented paradigm; this is where time is considered as small sequential slices at a selectable granularity (e.g. 1ms, 5ms, 10ms). For every simulation tick, the time-slice increments and any events that have occurred or are occurring within that time slice are handled. Unlike an event-driven approach, every time-slice is simulated, allowing for continuous receive behaviour close to that of a real-world scenario; the drawback being that it is processor intensive.

## 4.1.2   Radio Model

### 4.1.2.1   Transmitting

When a packet is transmitted, it is modelled in terms of start time, airtime and emanating location. Each time-slice the environment will poll each radio to collate all ongoing transmissions in the environment; this is the list which radios attempt to receive from and interference models are calculated for. If a radio's location changes between time-slices, the emanating location will be re-evaluated each time, however, the Doppler effect is not modelled because it has little effect for on LoRa at expected movement speeds [36]. Transmission airtimes are calculated using the equations detailed in Section 2.1.3.

### 4.1.2.2   Receiving

Every time-slice, a radio, provided it is not transmitting, will fill its receive buffer with a partial receive of the strongest receivable transmission (highest SNR) in the environment. For LoRa transmissions, receivable implies the same SF, BW and CF values are used. If multiple receivable signals are present, and the radio is not synchronised with a signal, the strongest will be captured. A small advantage is provided to favour receiving synchronised transmissions to support Class B and C collision scenarios. Class E collisions are handled by randomly adjusting receive SNRs slightly so that no preference is made between two signals with similar strength. Simulator collision results, as verified by the `TestCollision` class, are seen in Table 4.1.

TABLE 4.1: Results for collision scenarios defined in Table 2.3, when modelled in the simulator. All scenarios are modelled correctly for all SFs.

| ID | Status | Metadata Status |
|:--:|:------:|:---------------:|
| A | Receive A | SUCCESS |
| B | Receive A | SUCCESS |
| C | CRC Fail A | PAYLOAD_COLLISION |
| D | Collision | PREAMBLE_COLLISION |
| E | Collision | PAYLOAD_COLLISION |
| F | Receive A | SUCCESS |

Synchronisation is achieved when the important preamble of a signal is in the receive buffer and demodulated successfully. Attempted demodulation occurs at the end of each time-slice and must pass at three stages to successfully receive a signal. If any stage fails the latter stages will not occur, but the signal will be unreceivable and may still interfere. The stages are:

**S1** When a transmission's first important preamble symbol is seen. Start of synchronisation.

**S2** At the end of the transmission's preamble. At this point the radio is synchronised with a signal and is aware that it is receiving [6].

**S3** At the end of the transmission. Check for successful receive.

**S1** purely checks if the signal is strong enough using the radio's demodulation curve. Failure will result in `NO_PREAMBLE`, indicating a weak preamble. **S2** and **S3** also verify that enough of the transmission is present. This is required because it is possible that another powerful transmission has started filling the receive buffer – at this stage other signals are considered interference. For **S2**, 80% of the signal must be preamble from the correct signal. For **S3** the amount of interference must not exceed the CR's capability (Table 2.1); this resembles burst-interference disrupting a portion of the signal. Failure due to interference will result in a `PREAMBLE_COLLISION` or a `PAYLOAD_COLLISION` for **S2** and **S3** respectively. Likewise a demodulation failure will result in either `NO_PREAMBLE` or `WEAK_PAYLOAD`. These statuses are simulation metadata, the radio does not necessarily know the failure details or that it even occurred - a mapping of metadata to radio knowledge is seen in Table 4.2.

TABLE 4.2: Mappings of simulator receive statuses to those the radio would see.

| Metadata Status | Radio Status | Radio Aware |
|---|---|---|
| NO_PREAMBLE | N/A | No |
| PREAMBLE_COLLISION | Collision | Yes |
| WEAK_PAYLOAD | CRC Fail | Yes |
| PAYLOAD_COLLISION | CRC Fail | Yes |
| SUCCESS | Receive | Yes |

The mentioned demodulation curve varies depending on whether the theoretical model or the empirical RFM95W is used; only the latter is considered here. The transmission strength is calculated as the log-mean SNR of all its partial receives.

The corresponding $p = \text{PRP}^{\text{SF}}_{\text{SNR}}$ is found from the the best-fit sigmoid. If the SNR is close to $D_L$, $p$ is randomly adjusted to emulate high-variance behaviour. Demodulation success is then determined as a random chance with success $p$. The demodulation curves for receives at various SNRs are plotted in Figure 4.1 (output generated by `FreeSpacePlot` class).
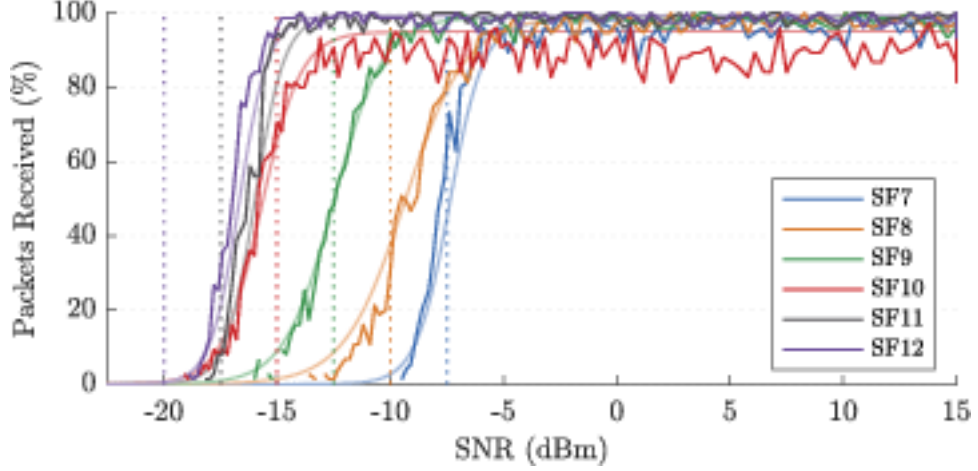


FIGURE 4.1: Simulator demodulation performance, assessed as PRP for increasing SNR. Each point is the result of 75 transmitted packets at the respective SNR. The faded lines indicate the empirical fit curves from Section 3.2.1.

### 4.1.2.3   CAD

LoRa's CAD process requires the ability to poll the receive buffer for a preamble symbol. When the process is invoked, the initial contents of the receive buffer are emptied as previous receive data cannot be used. A symbol's length of receive buffer is then captured (Equation 2.3a) and then the CAD search result is returned after the average processing time ($0.85 \cdot S_T$) [6]. Activity is detected if at least 80% of the receives in the buffer are preamble and a standard demodulation curve check passes. When the process is complete the full receive buffer is dumped.

## 4.1.3   RPS ($R_P$) & SNR Model

The actual receivable signal power of a transmission is derived from the link budget equation, Equation 4.1 explicitly repeats this for the factors modelled.

$$R_P = TX_{power} + TX_{gain} + RX_{gain} - P^{TX \rightarrow RX}_{loss} \tag{4.1}$$

Gains at the receiver and transmitter end are broken down into fixed antenna gains and cable losses. The path loss ($P_{loss}$) is broken down into free-space loss and object loss. A global free-space model is used for the environment, selectable at creation; built-in options include those defined in Section 3.2.2: E-FSPL, FSPL, PE.
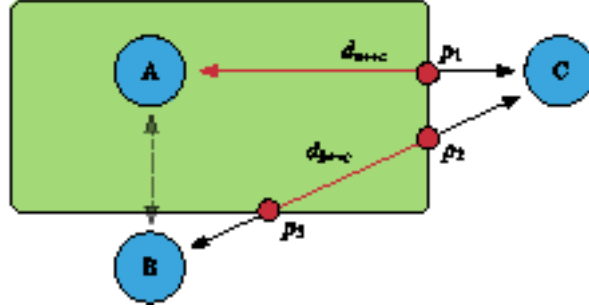


FIGURE 4.2: Scenarios for LOS path loss whilst passing through objects.

Objects are entities in the environment, which will possess their own propagation model; built-in models include: COST235, Weissberger and the ITU-R. Forests are a type of built-in object; these can take any 2D shape and use the ITU-R model with a $\beta$ multiplier. All this combined allows the path loss curves from Section 3.2.2 to be recreated. Of course in a real environment, it is likely that not all radio transmissions will pass through the same obstacles. There is no perfect way to handle this, the closest would be the one woodland terminal model [37] but this sets severe limits; one radio must be in the object and the other outside with no other obstacles in the path. Therefore a more approximate approach is taken. In short the total $P_{loss}$ is sum of the free-space loss and the segment of the propagation curve from the obstacle. Using Figure 4.2 as a scenario reference, the following are examples of extra $P_{loss}$ due to obstacles. Equation 4.2 calculates for $A \leftrightarrow C$ where one radio is in the obstacle.

$$P_{loss \text{ (Object)}}^{A \to C} = P_{loss}^{A \to p_1} \quad \leftrightarrow \quad P_{loss \text{ (Object)}}^{C \to A} = P_{loss}^{C \to A} - P_{loss}^{C \to p_1} \qquad (4.2)$$

Equation 4.3 calculates for $B \leftrightarrow C$ where the transmission completely passes through the object.

$$P_{loss \text{ (Object)}}^{B \to C} = P_{loss}^{B \to p_2} - P_{loss}^{B \to p_3} \quad \leftrightarrow \quad P_{loss \text{ (Object)}}^{C \to B} = P_{loss}^{C \to p_3} - P_{loss}^{C \to p_2} \qquad (4.3)$$

As the method has large swings in path loss depending on whether obstacles are close to the receiver or transmitter, $\max(P_{loss}^{TX \to RX}, P_{loss}^{RX \to TX})$ is taken; this means path loss will be the same regardless of the transmission direction – interference

differences may still mean that SNR varies. The model scales to any number of objects in the path. Note that fast-fading is abstracted into the demodulation curve of the receiver and is not modelled separately.

The channel power as seen by a receiver (RSSI) at a location, is modelled as the sum of: all 'interfering' signal powers, the thermal noise floor, and the receiver noise figure. When attempting to receive a signal, its observed $R_P$ can removed from the RSSI calculation to provide the channel noise ($N$). The SNR can then be calculated as $R_P - N$. Interfering sources, narrowband or otherwise, are considered as those where the bandwidth used overlaps with the receive channel. As per LoRa's orthogonality defined in Section 2.1.6, a LoRa transmission is only considered to interfere if the chirp rate is the same as that of the receive configuration.

### 4.1.4   Protocol Testing Infrastructure

Protocols are implemented the layer above the low-level radio behaviour using a listener infrastructure. When the time-slice increments, first the raw radio behaviour will occur, and then a 'tick' process will be called on any listeners. These listeners maintain their own state between ticks allowing them to schedule transmissions and handle received packets, ultimately allowing emulation of a full protocol stack. This is how all the protocols defined in Section 5 are implemented. The base listener class, `ProtocolTickListener`, provides methods for directly handling events that have occurred the previous tick (synchronisations, receives), and handles protocol performance tracking. Statistics can be dumped with a by-radio perspective or a by-transmission perspective and can be filtered to disregard failures of transmissions that are not 'wanted' by a receiver (see Section 5.1).

The execution of an environment (and the radios within it) is handled by an `EnvironmentRunner`; this can step time by the configured granularity a number of times or run continuously. Execution occurs on a separate thread and employs listeners to allow external interaction either through a test harness or GUI. Events can be scheduled for execution at fixed times to allow for scripted test behaviour; there is built-in support for radio movement, sending transmissions and verifying expected radio state; though, any custom behaviour can be implemented.

## 4.2   Interface (GUI)

The Java Swing interface acts largely as a wrapper for managing an `Environment Runner` and displaying the environment being executed. The full interface can be seen in Figure 4.3 with a brief explanation and further examples in Appendix F.
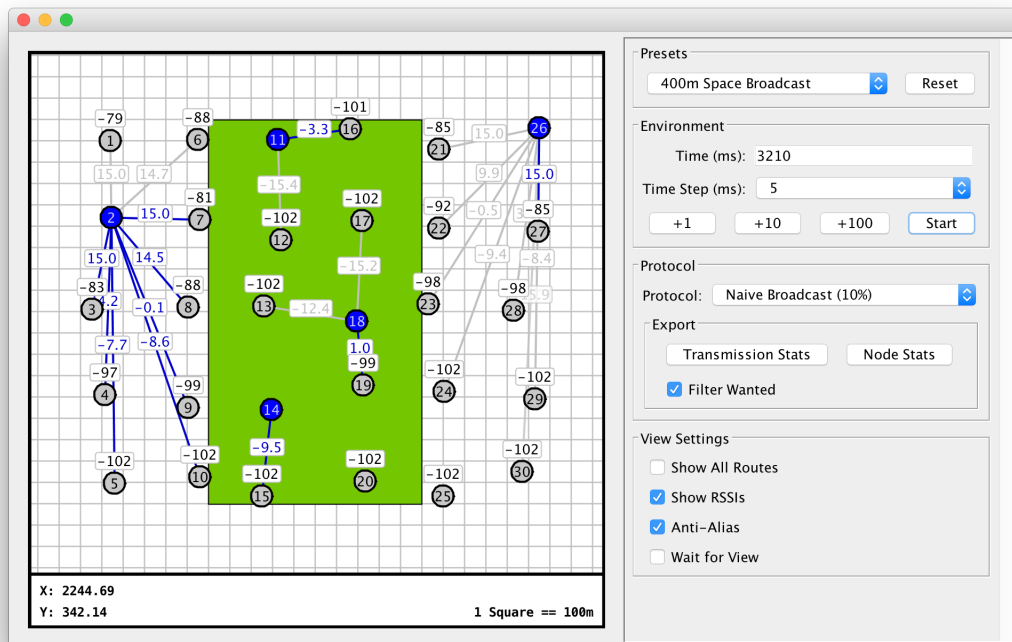


FIGURE 4.3: Simulator's GUI interface running the ALOHA protocol.

# Chapter 5

# MAC Protocols

In this section three contention-based MAC protocols are considered to handle the requirement of data transfers to physically close neighbours: a base case (ALOHA), a common approach (CSMA) and a scenario specific approach (LLBP).

## 5.1 Considerations

Designing approaches so that as many radios as possible receive a transmission is of little help; from the receiver's perspective, if local-interest data is received 1500m away, the transmission is unwanted and increasing the chance of a local collision. To this end a criteria is defined as the maximum distance for which data is 'wanted'; this is set to the worst-case transmission distance (500m).

The LoRa configurations used are the abstracted DRs from LoRaWAN [10]; however, DR0 and DR2 are disregarded due to their lack of respective SF performance. Although small packets ($< 20$ bytes) have been shown to have slightly higher receive probability, they are not practical with transmission overhead, therefore packets are allowed to be any size ($\leq 255$ *bytes*). CR and TPs are assumed to be 4/5 and 14dBm respectively.

As opposed to LoRaWAN's DC manager (see Figure 2.3), all protocols use a custom DC manager proposed in Appendix G. This is more flexible because it considers airtime over the full enforcement interval ($d_i$), allowing multiple sequential transmissions without silence; this is a requirement for bulk transmissions or protocol handshakes.

## 5.2   Approaches

### 5.2.1   ALOHA

Uses LoRaWAN's principle of sending data periodically provided the DC limit allows. No carrier-sensing is carried out, but transmissions will be delayed if the transmitter is receiving at the scheduled time. For purposes of testing, the minimum spacing between transmissions is that enforced by LoRaWAN. Therefore, in the case that any backoff occurs, less than the DC's maximum worth of data will be transmitted. MAC performance purely relies on each radio only using a small amount of airtime. As all radios must be on the same configuration the method can only use a single channel and DR – no mechanism is used for dynamically agreeing parameter changes. Consequently, a fixed DC of up to 10% is supported on band h1.6. Test packets use random payload sizes and all packets are treated as data.

### 5.2.2   CSMA

Uses the ALOHA approach but does carrier-sensing using LoRa's CAD process immediately before transmissions. On detection, random backoff will occur before the CAD process repeats; this is a simplified approach to that proposed in [16]. The PSs are increased from 8 to 32 to increase preamble detection likelihood with the drawback of increased airtime overhead. When all nodes are within range of one another the vulnerable collision period is very short; provided no failed synchronisations take place, collisions should only occur if two transmitter's CADs overlap; collisions resulting from the hidden node problem (Figure 5.1) are not avoided.
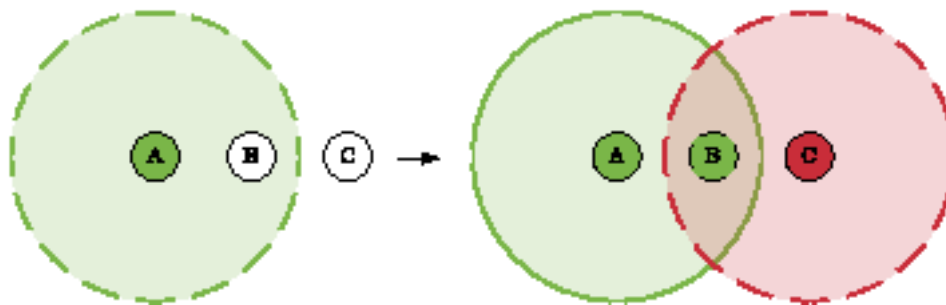


FIGURE 5.1: Demonstration of the hidden node problem. A has transmitted before C, however, C was unable to sense A and assumes it is okay to transmit, resulting in a collision at B [26].

## 5.2.3   LoRa Local Broadcast Protocol (LLBP)

This is a bespoke approach that makes use of dynamic channel and SF switching with the target of constricting receivability to local listeners. The protocol uses two bands: a management-band (h1.4) and a data-band (h1.3). The former is treated as a single CSMA channel, whereas the latter allocates 15 channels at CFs $865.1 + 0.2 \cdot C_n$ (BW=125kHz).

In principle, the protocol announces when a transmitter has a large chunk of data to send using a data announcement packet (DAP); this contains the LoRa configuration to switch to and a description of the data being sent (Figure 5.2). When a radio receives this packet it can make its own decision on whether it wants the data; if it does not it can ignore the message and will never see any data packets, otherwise it can switch configurations and only see those packets. This dump behaviour is heavily suited to SCF situations.
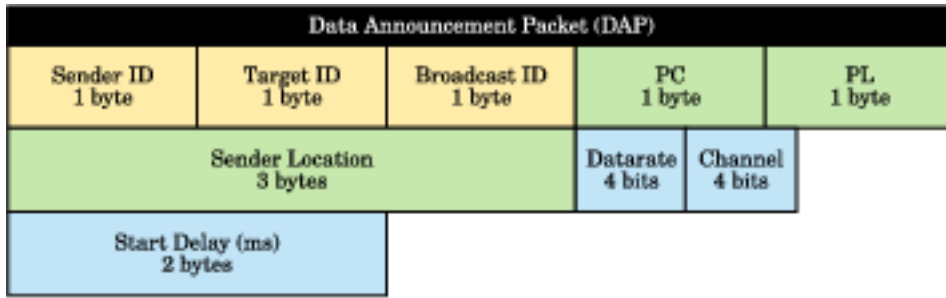


FIGURE 5.2: DAP structure. The number of data packets being sent and their average length is provided so the receiver can timeout appropriately in case no packets arrive. The delay field is provided to indicate the relative start time to allow multiple DAPs. The target can be set to make announcements unicast.

As opposed to agreeing the configuration with a flurry of transmissions at one point, the configuration is decided by the transmitter, using its prior knowledge of surrounding transmitters. This knowledge is gained through periodical heartbeat packets (Figure 5.3), sent on the management-band; these provide SNRs and locations. The fastest viable DR is picked along with a random data-band channel. There is no guarantee the channel is free but with the number of available channels, and a compulsory 1% DC across all of them, collisions are unlikely. DR is selected such that for wanting receivers $\min(\text{SNR}) > (D_L + 2.5)$; this is where PRP should be approximately 100%. The side effect of choosing the fastest DR is less airtime; although this could be used to achieve more throughput, instead it is used to keep interference times to a minimum for the same data.

| Heartbeat Packet | | |
|---|---|---|
| Sender ID 1 byte | Sender Location 3 bytes | Optional Payload ··· |
| | ··· | |

FIGURE 5.3: Heartbeat structure. Transmits a sender's location with SNR inferred. A payload can be attached to avoid wasted overhead.

## 5.3    Test Methodology

Protocol testing was executed on one of the simulator environment presets, `LargeData BroadcastTest`. The preset provided automatic generation of an $[x \times y]$ radio grid where spacing ($S$) was the same $\pm 20\%$. It provided four obstruction options seen in Figure 5.4.
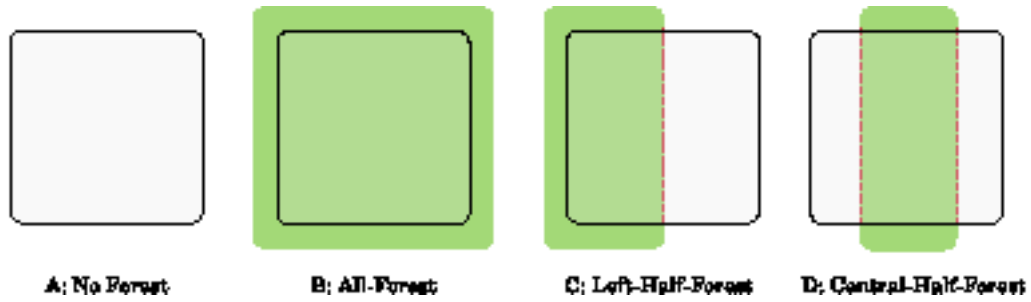


FIGURE 5.4: `LargeDataBroadcastTest` obstruction options, green indicates forest where $\beta = 0.55$. Radios are scattered in the black square

If radios were always able to use their fastest configuration, it was unlikely a protocol with overhead would outperform one without. To alleviate this unfairness, $S$ was set to 400m; ensuring that in-forest radios needed DR1 to communicate, but giving other transmissions the opportunity to increase DR.

The protocol configurations executed for each environment were:

- ALOHA with DCs of 1% [A] and 10% [B].

- CSMA with DCs of 1% [C] and 10% [D].

- LLBP with DAP count of 1 [E] and 2 [F].

- LLBP with DAP count of 1 where true locations and SNR values were known [G]. This can be considered as LLBP's best case performance but is not representative of actual performance.

For LLBP heartbeats were sent for 1/2 of the management-band airtime. 1/6th of the data-band airtime was sent after each DAP; meaning 6 DAPs an hour. Movement was not simulated but received heartbeats timed out after 10 minutes to reflect that movement is expected.

Each of the 28 configurations was executed in the simulator for 6 hours of simulation time, after which simulator statistics were exported.

## 5.4   Results & Discussion

Each protocol is assessed by: its throughput of *wanted* data per transmitter over the simulation period ($T$) and the delivery percentage (DP). Together giving an understanding of the effective throughput. Aggregated results are seen in Figure 5.1 with separated box-plots of the two metrics in Figure 5.5 and Figure 5.6 respectively.

TABLE 5.1: Results aggregated by protocol, taking the mean of each transmitter across all environments.

| Configuration | Throughput (KB) | DP (%) |
|:---:|:---:|:---:|
| **A** | 35 | 91 |
| **B** | 203 | 69 |
| **C** | 30 | 91 |
| **D** | 183 | 77 |
| **E** | 18 | 47 |
| **F** | 34 | 52 |
| **G** | 31 | 86 |

Unsurprisingly, throughputs are clustered by DC, where $T_{10\%} \gg T_{1\%}$. It could be expected that $10\times$ the DC would result in $10\times$ the throughput; however the actual increase for both ALOHA and CSMA is approximately $6\times$. The other $4\times$ accounted for by: backoff from the cluttered airspace (ALOHA = $1.9\times$, CSMA = $2.5\times$), and more frequent failed/missed receives (ALOHA = $2.3\times$, CSMA = $1.4\times$). Low DP, as a result of collisions and busy receivers, leads to unpredictability, increasing overhead caused by acknowledgements and retransmissions. The drops in DP for A $\rightarrow$ B and C $\rightarrow$ D are 22% and 14%. If these dropped packets require retransmissions, without considering acknowledgements, effective throughput drops to 47% and 63% respectively; considerations like these are implementation specific. Even given these

arguments, effective throughput will usually improve by increasing DC though more testing is required to find the limit. The 10% drop in throughput and 8% increase in DP for B → D indicates that CSMA is only worth the overhead when taking retransmissions into account - if guaranteed receives are not required, ALOHA is more efficient.
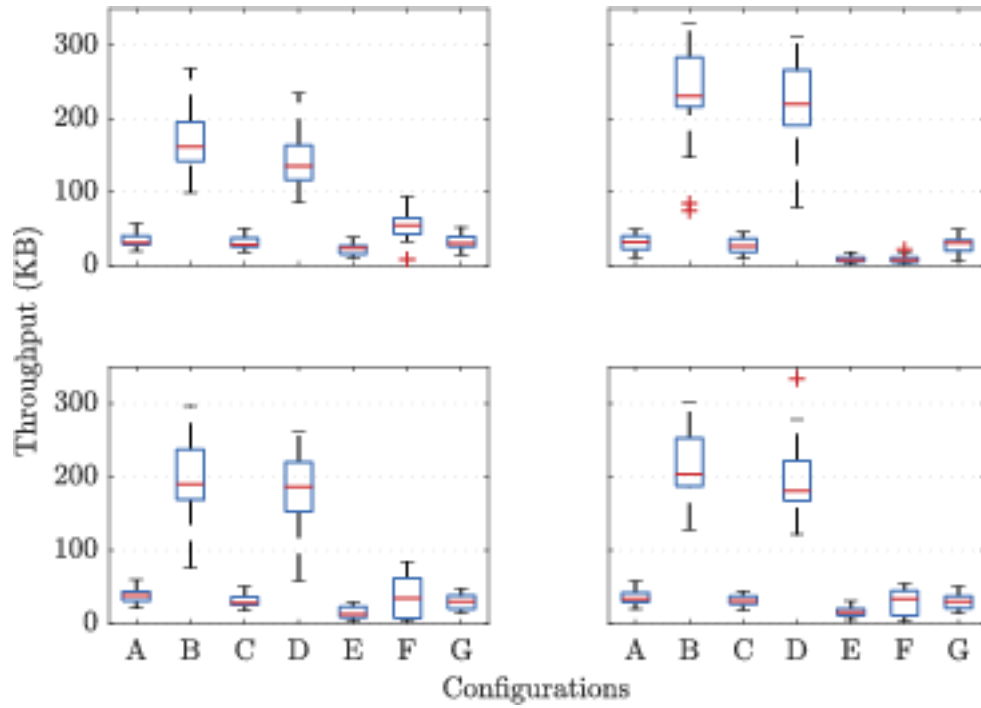


FIGURE 5.5: Box-plots of each transmitter's throughput in each environment [[A, B], [C, D]]. They demonstrate the throughput advantage of higher duty cycles and with that, higher variance between individual transmitter's access to the medium.

With this established, direct comparisons cannot be made between LLBP and configurations with 10% DCs. However, it is immediately clear that the *fair* LLBP implementations do not out perform the 1% ALOHA and CSMA configurations; as is demonstrated by $P_{E||F} \ll P_{A||C}$ and $T_{E||F} \leq T_{A||C}$. Even with the best (*cheat*) LLBP case, G has significantly less DP than the simpler approaches. Figure 5.7 indicates that the receiver can often not see data packets for LLBP configurations, indicating that the receiver does not switch bands correctly. This is likely caused by DAP receive failures; the theory made more likely by the significant increase of DP ($p = 0.01$) for E → F. This issue is likely due to less critical heartbeat packets colliding with DAPs.

That being said, the far more significant problem can be seen by comparing E to G. G uses the same DAP count but has perfect data for DR selection. The increase in performance indicates that transmitter decisions made by E/F are not informed by enough data, resulting in an overly aggressive DRs being selected. These problems could be remedied by: increasing the heartbeat timeout, though this will slow down topology updates, or making heartbeats more frequent/descriptive, though this will increase DAP loss chance. To facilitate these changes the management-band could be switched to h1.6 (DR=10%), though this removes the possibility of having a separate high-rate channel for critical communications.
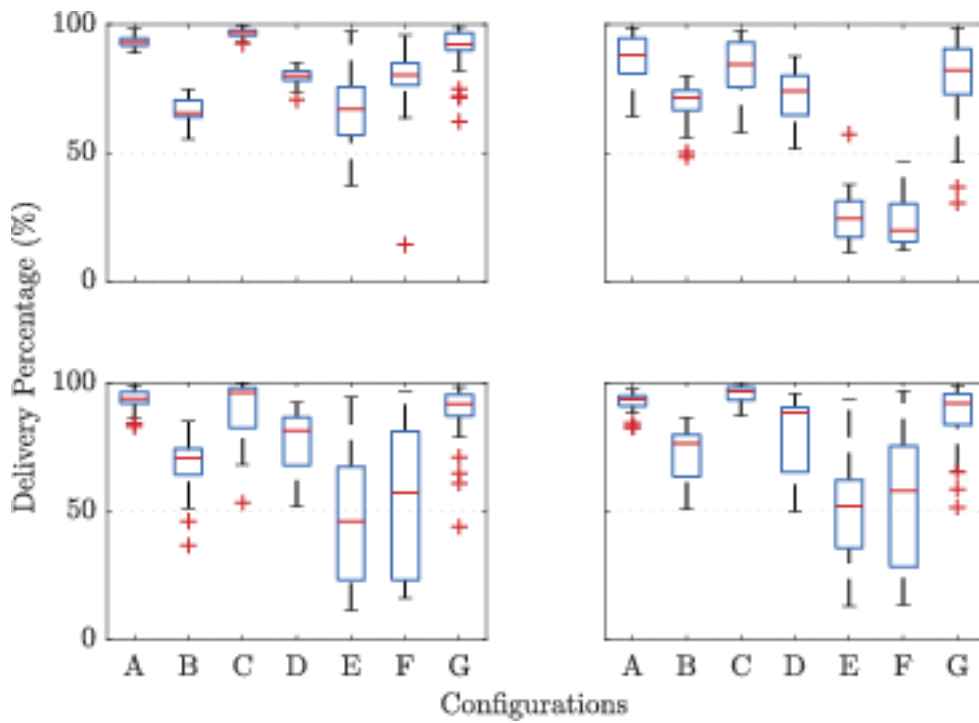


FIGURE 5.6: Box-plots of DP in each environment [[A, B], [C, D]]. Highlighted is the consistency of ALOHA and CSMA between environments. LLBP's failings to select the correct DR are highlighted by it only having acceptable performance in Environment A where any DR will do.
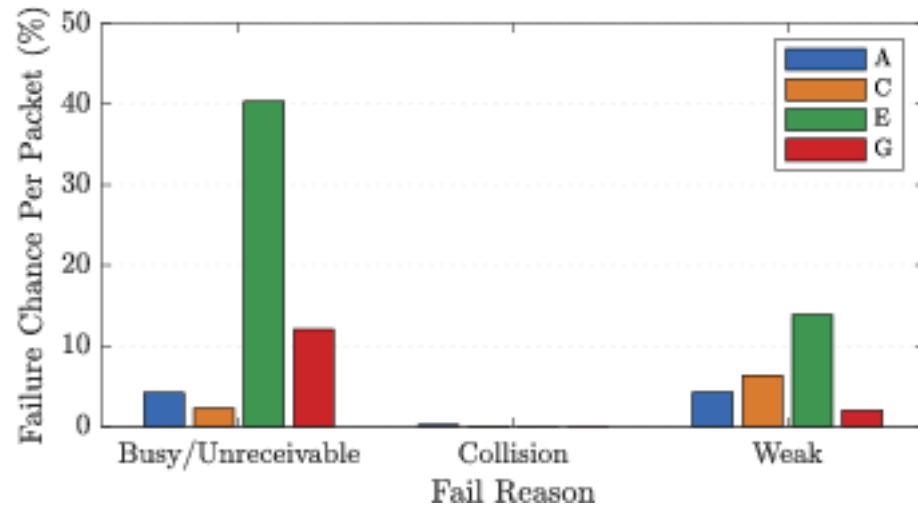
FIGURE 5.7: Number of packet failures per configuration normalised by number of possible packet failures. Busy failures may have occurred due to the receiver: being synchronised with a stronger signal, doing CAD or being on the wrong configuration. Some collisions are recorded as weak due to general noise increases reducing demodulation success.

# Chapter 6

# Conclusion

This paper has presented an assessment of LoRa for sparse swarm scenarios covering: physical radio performance, regulation concessions, and how that maps to prospective MAC protocol performance. Conclusions are that LoRa's physical technology is suitable with recorded transmit ranges, using typical LoRa radios, far exceeding that achievable by Wi-Fi or other comparable technologies – 1600m in free-space or 500m in high-propagation forest can be expected even with scenario compromises.

That being said, given its naturally low-data-rate, the technology is severely handicapped by Sub-1GHz band limitations in Europe. Future work could study the more freely regulated 2.4GHz LoRa implementation, though this is unlikely to be applicable to forest scenarios. The usable unicast throughput of ∼15KB per hour (∼2.5KB if multiple channels are required), whilst conforming to regulation is significantly worse than can be expected from usual swarm transfer mediums. LoRa's multiple data-rate configurations could alleviate this, either through manual configuration on a deployment basis, or through a MAC protocol.

The attempts in this paper to create said protocol were ultimately unsuccessful, with basic ALOHA and CSMA approaches outperforming the proposed LLBP. A variation on LLBP with slotting or minor tweaks may be able to deliver better/equal performance, or a contention-free Mobile-LMAC [26] like approach may be required. The potential of new cheaper gateway devices could help deliver a solution to this problem but this is all a topic for future research.

Though overall the created simulator provided a reasonable assessment of protocols and proposed some novel modelling techniques to closely emulate real-world context, one drawback of the testing approach was that decisions were made mostly agnostic

to scenario data. Given MAC layers can be very scenario specific, implementing realistic swarm data models and distribution algorithms like SOUL [3] would give more relatable between-protocol assessment. The protocol may need to be fully integrated into a network stack, e.g. with routing protocols, for this. Ultimately, this should lead to real-world verification with radio hardware; the proposed logging platform would be suitable for this.